Surface exclusion of IncC conjugative plasmids and their relatives

Nicolas Rivard[1], Malika Humbert[1¶], Kévin T. Huguet[1#a¶], César Pérez Bucio[2], Eve Quirion[1], Vincent Burrus[1*]

[1]Département de biologie, Université de Sherbrooke, Sherbrooke, Quebec, Canada

[2]Instituto Tecnológico y de Estudios Superiores de Monterrey, Monterrey, Nuevo León, Mexico

[#a]Current address: Centre international de recherche en infectiologie, Lyon, France

Short title: Surface exclusion of IncC conjugative plasmids

*Corresponding author

E-mail: Vincent.Burrus@USherbrooke.ca

¶These authors contributed equally to this work.

Abstract

The phenomenon of exclusion allows conjugative plasmids to selectively impede the entry of identical or related elements into their host cell to prevent the resulting instability. Entry exclusion blocks DNA translocation into the recipient cell, whereas surface exclusion destabilizes the mating pair. IncC conjugative plasmids largely contribute to the dissemination of antibiotic-resistance genes in Gammaproteobacteria. IncC plasmids are known to exert exclusion against their relatives, including IncC and IncA plasmids, yet the entry exclusion factor *eexC* alone does not account for the totality of the exclusion phenotype. In this study, a transposon-directed insertion sequencing approach identified *sfx* as necessary and sufficient for the remaining exclusion phenotype. Sfx is a novel exclusion factor unrelated to the ones described to date. A cell fractionation assay localized Sfx in the outer membrane. Reverse transcription PCR and beta-galactosidase experiments showed that *sfx* is expressed constitutively at a higher level than *eexC*. A search in Gammaproteobacteria genomes identified Sfx homologs encoded by IncC, IncA and related, untyped conjugative plasmids and a novel family of integrative and mobilizable elements that likely rely on IncC plasmids for their mobility. Mating assays demonstrated that *sfx* is not required in the donor for exclusion, ruling out Sfx as the exclusion target. Instead, complementation assays revealed that the putative adhesin TraN in the donor is the target of surface exclusion. Mating assays with TraN homologs from related untyped plasmids from *Aeromonas* spp. and *Photobacterium damselae* identified two surface exclusion groups, with each Sfx targeting TraN homologs from the same group. Together, these results allow us to understand better the apparent incompatibility between IncA and IncC plasmids and to propose a mechanistic model for surface exclusion mediated by Sfx in IncC plasmids and related elements, with implications for the rampant dissemination of antibiotic resistance.

Author summary

Bacterial conjugation plays a pivotal role in the evolution of bacterial populations. The circulation of drug resistance genes bolsters the emergence of multidrug-resistant pathogens, with which contemporary medicine struggles to cope. Exclusion is a natural process preventing the redundant acquisition of a plasmid via conjugation by a host harbouring an identical or similar plasmid. Although exclusion has been known for the past half-century, the mechanisms involved remain poorly understood. This study describes a novel exclusion factor, Sfx, encoded by IncC, IncA and related conjugative plasmids and by unrelated integrative and mobilizable elements. We report that Sfx is a lipoprotein of the recipient that selectively inhibits conjugation based on the adhesin TraN expressed at the surface of the donor. We propose a mechanistic model for Sfx-mediated exclusion. Ultimately, a better understanding of exclusion could facilitate the design of novel conjugation inhibitors targeting mating pair formation to curb the circulation of drug-resistance genes in healthcare settings, agriculture, animal husbandry and food and drug production.

60 **Introduction**

61 IncC plasmids are large conjugative plasmids frequently associated with multidrug resistance
62 phenotypes in a broad range of Gammaproteobacteria species [1]. IncC plasmids' ability to
63 mobilize non-autonomous, unrelated integrative and mobilizable elements (IMEs) of the SGI1
64 and MGI*Vch*Hai6 families exacerbates their importance in antibiotic resistance dissemination
65 [2–5]. IncC, IncA and untyped IncA/C-like (ACL) plasmids (e.g., pAsa4c, pAhD4-1, pAQU1)
66 share a syntenic set of genes involved in conjugation, DNA repair, and regulation. All seem
67 regulated by closely related homologs of the master activator of transfer AcaCD [6–8]. IncC
68 plasmid-encoded AcaCD promotes the excision and mobilization of MGI*Vch*Hai6-like IMEs [4,5].
69 AcaCD also stimulates the excision and replication of SGI1 and the expression of its *traN*, *traG*
70 and *traH* genes, which modify the mating apparatus of IncC plasmids to enhance its
71 dissemination [6,9,10].
72 Large conjugative plasmids are autonomous replicons that usually remain at a low-copy
73 number. The entry into the same cell of a plasmid sharing similar replication or partitioning
74 determinants promotes plasmid destabilization and loss, a phenomenon known as
75 incompatibility [11]. Exclusion refers to the mechanisms employed by conjugative elements to
76 preclude instability resulting from incompatibility by hindering redundant transfer into the cells
77 they reside [12]. While the definite nature of exclusion mechanisms remains elusive, they can
78 be categorized as entry and surface exclusion by whether they interfere with DNA transfer or
79 mating pair stabilization [12,13]. Exclusion seems to be a staple of the conjugative plasmid
80 lifestyle. Exclusion factors have been identified in the IncF, IncHI1, IncI, IncN, IncP, IncW and
81 ColE1 families, plasmids of the pKPC_UVA01 replicon type and the enterococcal conjugative
82 plasmid pCF10 [13–21]. Integrative and conjugative elements (ICEs) of the SXT/R391 family
83 and ICE*Bs*1 of *Bacillus subtilis* also encode exclusion determinants [22,23]. Most exclusion

84 factors identified to date are associated with the cytoplasmic membrane, where they would exert
85 entry exclusion, with only the IncF TraT firmly established as a surface exclusion factor [12,13].
86 Like TraT, the IncHI1 EexB localizes in the outer membrane and is thought to engage in surface
87 exclusion [14]. Likewise, the surface-exposed PrgA protease of pCF10 reduces aggregation and
88 transfer [21].
89 Exclusion is not specific to the transferred DNA [24], and proteins in the donor have been
90 identified as targets of exclusion factors in several systems. EexA and EexB of IncHI1 plasmids
91 and TrbK of pKPK_UVA01 appear to act concurrently as exclusion factors and exclusion
92 targets, as they are necessary in both the donor and recipient for exclusion to take place
93 [14,20]. Other exclusion factors target different plasmid-encoded proteins. The IncI ExcA targets
94 TraY, which is found in the cytoplasmic membrane of the donor [15]. Similarly, the IncF TraS
95 and SXT/R391 Eex of the recipient seem to interact directly with the VirB6 homolog TraG of the
96 donor, and the regions involved in both proteins are cytoplasmic [22,25]. In the cases above, the
97 genes encoding the exclusion factor and its target are adjacent. In IncP, IncW and IncN
98 plasmids, for which the exclusion target remains unknown, the exclusion gene abuts a gene
99 coding for a VirB6 homolog, suggesting a widespread usage of this target beyond the IncF and
100 SXT/R391 families [12].
101 The surface exclusion factor TraT of IncF plasmids reduces the percentage of mating
102 aggregates, and five contiguous residues determine specificity between exclusion groups
103 [13,26]. Harrison *et al*. proposed that TraT destabilizes the mating pair by interacting with the
104 pilus tip; however, it was eventually shown that the pilin does not define exclusion specificity
105 [26,27]. The discovery of interactions between TraT and the outer membrane protein OmpA in
106 the recipient and between OmpA in the recipient and the putative adhesin TraN in the donor
107 suggested surface exclusion could instead result from TraT preventing docking of TraN to

108 OmpA, thus hindering mating pair stabilization [28–30]. The identification of TraN receptor
109 specificity groups across IncF plasmids makes this hypothesis extremely appealing, yet *traN*
110 substitutions failed to flip exclusion specificity between F and R100-1 [29,31,32].
111 IncC plasmids share with IncA plasmids the same entry exclusion system, *eexC*/*traG*, and
112 inhibit each other's entry into the cell in which they reside [8,33]. During the characterization of
113 *eexC*/*traG*, we reported that knocking-out *eexC* of the IncC plasmid pVCR94 in the recipient
114 only reduced the exclusion phenotype in mating assays using an IncC$^+$ donor. Likewise, the
115 deletion of a 45.6-kb fragment encompassing 33 open reading frames located between *traN* and
116 *traF* led to a statistically significant reduction of exclusion. Hence, another mechanism likely
117 prevents redundant transfer between cells containing identical plasmids.
118 In this report, we investigate the cause of the incomplete abolition of exclusion by a recipient
119 strain bearing an IncC plasmid lacking the entry exclusion gene *eexC*. Using a transposon-
120 directed insertion sequencing (TraDIS) approach, we identified IncC-borne candidate genes
121 whose disruption in recipient cells facilitated the acquisition of an incoming mobilizable plasmid
122 from an IncC$^+$ donor. Further analyses revealed that a single open reading frame, hereafter
123 named *sfx*, flanked by *traN* and *acaB*, accounts for the residual exclusion phenotype. Deletion
124 of *sfx* with *eexC* completely abolished exclusion. Signal peptide prediction and a subcellular
125 localization assay suggest the Sfx protein is an outer-membrane lipoprotein and support a role
126 as a surface exclusion factor. Sfx belongs to a novel family of broadly distributed surface
127 exclusion proteins encoded by IncC plasmids, their relatives and several putative IMEs. Surface
128 exclusion assays designed to test *sfx*/*traN* gene pairs from ACL plasmids revealed that *sfx* and
129 *traN* are part of a surface exclusion system, enabling us to propose a model of surface
130 exclusion of ACL plasmids.
131

132 ## Results

133 ### *vcrx085* impedes conjugative transfer between IncC$^+$ cells

134 To identify additional factors responsible for the inhibition of transfer between IncC$^+$ cells, we
135 constructed a high-density Tn*5* insertion library in *E. coli* GG56 carrying pVCR94^{Kn} Δ*eexC*::*cat*,
136 a kanamycin-resistant variant of pVCR94 unable to exert entry exclusion in recipient cells [8].
137 This set of mutants formed the input library enriched in Tn*5* insertions that allowed plasmid
138 replication and maintenance. The input library became the recipient in a mating assay with a
139 donor strain carrying pVCR94^{Kn} and the mobilizable plasmid pClo (Fig 1A). GG56
140 transconjugant colonies that acquired pClo made up the output library. We expected that genes
141 or sequences of pVCR94^{Kn} Δ*eexC*::*cat* more frequently disrupted in the output than in the input
142 (high insertion index ratio) were those impeding the mobilization of pClo between IncC$^+$ cells.
143 Of nine candidate genes with insertion index ratios above the arbitrary threshold of 5 (Table 1,
144 Fig 1C, S1 Fig), only *acr2* (*vcrx150*) is a known repressor of conjugative transfer [6]. To validate
145 the ability of the candidates to inhibit incoming conjugative transfer, we tested corresponding
146 deletion mutants of pVCR94^{Sp} used as recipients in mating assays. All but one had no impact
147 on transfer (Fig 1D). The deletion of *vcrx085* (hereafter referred to as *sfx* for surface exclusion)
148 improved conjugation to a level similar to the deletion of the entry exclusion factor *eexC*. Like
149 *eexC*, we could complement the *sfx* deletion in *trans*. Both mutations combined completely
150 abolished exclusion, allowing conjugation to a level comparable to an empty recipient.

151 **Table 1. Candidate genes identified by TraDIS.**

ORF	Fold change	Predicted size (aa)	Predicted product[a]
vcrx018	6.39	119	Hypothetical protein
vcrx019	5.17	148	$Fe3^+$-siderophore ABC transporter permease
vcrx062	8.67	194	Hypothetical protein
vcrx085 (*sfx*)	6.22	286	Lipoprotein (Sec/SPII)

vcrx107	6.07	114	Hypothetical protein
vcrx108	6.08	100	Hypothetical protein
vcrx111	6.83	184	Hypothetical protein
vcrx137	6.63	163	Hypothetical protein
acr2	6.50	139	Transcriptional repressor

152 [a]As predicted by NCBI blastp or SignalP 6.0.

153 **Sfx is a constitutively expressed outer membrane protein**

154 The predicted translation product of *sfx* contains a lipoprotein signal peptide (S2 Fig),
155 suggesting it is displayed on the cell surface [34]. A C-terminally 3xFLAG-tagged version of *sfx*
156 was cloned under the control of the inducible promoter P_{tac}. The Sfx-3xFLAG polypeptide has a
157 predicted size of 33.4 kDa before signal peptide cleavage and 31.7 kDa afterwards. A cell
158 fractionation assay confirmed the presence of Sfx-3xFLAG in the outer membrane fraction (Fig
159 2AB). This cellular location is consistent with the role of Sfx in surface exclusion. We could not
160 undoubtedly assign the processed and unprocessed forms in the total cell extract, and an
161 additional product appeared between 25 and 30 kDa on the western blot. This weaker band is
162 presumably a degradation product of unknown nature.
163 *sfx* is located downstream of the transfer activator *acaB*, which is expressed from an AcaCD-
164 inducible promoter. Hence, we wondered whether *sfx* expression was controlled by AcaCD (Fig
165 2C) [35]. To test this hypothesis, we constructed a translational fusion between the third codon
166 of *sfx* and the eighth codon of *lacZ* in pVCR94^{Kn}. Expression of AcaCD did not impact the β-
167 galactosidase activity of the *sfx'-'lacZ* fusion. A similarly constructed *eexC'-'lacZ* fusion yielded a
168 ~150-fold lower β-galactosidase activity (Fig 2EF). Furthermore, to test whether *sfx* and *acaB*
169 are part of the same transcript, we attempted to amplify both loci from a cDNA synthesized from
170 the 3' end of *sfx*. While *sfx* could be amplified regardless of AcaCD, *acaB* remained
171 undetectable, suggesting that these two genes are expressed as independent mRNA transcripts
172 (Fig 2D). A Rho-independent terminator predicted between *sfx* and *acaB* supports this idea (Fig

173 2C, S2 Fig B). Altogether, our results indicate that *sfx* is constitutively expressed independently
174 of AcaCD at a much higher level than *eexC*.

175 **Genes encoding homologs of Sfx_{94} are found in diverse genomic backgrounds**

176 To explore the diversity of exclusion factors, we first used NCBI tblastn to identify Sfx_{94}
177 homologs in the ACL plasmids pAsa4c of *Aeromonas salmonicida* and pAhD4-1 of *Aeromonas*
178 *hydrophila*, and in the distant ACL plasmid pAQU1 of *Photobacterium damselae* ($traN_{AQU1}$) that
179 are known untyped relatives of IncA and IncC plasmids [7,8]. For pAsa4c and pAhD4-1, closely
180 related homologs were found adjacent to the gene *traN*. For pAQU1, the search resulted in a
181 single hit (*215*, hereafter referred to as sfx_{AQU1}) whose product shares only 39% identity over
182 273 amino acid residues with Sfx_{94}. sfx_{AQU1} is surrounded by genes of unknown function. Sfx_{AQU1}
183 was manually added to the dataset for downstream analyses. We next searched the GenBank
184 database for homologs of Sfx_{94} and extracted the resulting sequences for further analyses. 130
185 unique proteins were identified (S3 File), most encoded by ACL plasmids (Fig 3A). 78 Sfx
186 homologs share more than 90% identity with Sfx_{94}, including nine variants encoded by IncC
187 plasmids. All of the Sfx homologs encoded by IncC plasmids are inside this cluster. Sfx_{94}
188 belongs to an identical protein group of 193 representatives, all encoded by IncC or putative
189 IncC plasmids. Sfx_{RA1} from the IncA plasmid pRA1 belongs to the Sfx_{94} cluster as they share
190 92% identity over 286 amino acid residues. All plasmids outside the Sfx_{94} cluster are ACL
191 plasmids, including pAsa4c and pAhD4-1. In most ACL plasmids and with the rare exception of
192 pAQU1, *sfx* lies downstream of the *dsbC-traC-trhF-traWU* operon between *traN* and the transfer
193 activator gene *acaB* (Fig 3C).
194 The remaining Sfx proteins are encoded by putative IMEs integrated at four distinct
195 chromosomal locations. First, ten of these IMEs belong to the MGI*Vch*Hai6 family and are
196 integrated at the 5' end of *dusA* in environmental and clinical *Aeromonas* strains [5].

197 Represented by IE*Ave*Tha1 (Fig 3C), all possess MGI*Vch*Hai6-like *mobI* and *oriT* and predicted
198 AcaCD-responsive promoters. A second group represented by IE*Vch*Aut1 comprises six IMEs
199 integrated at the 3' end of *yicC* in environmental and clinical *Vibrio* strains. In addition to a
200 putative recombination directionality factor related to RdfM of MGI*Vfl*Ind1 [36], these IMEs carry
201 a set of conserved genes, including a predicted type IV coupling protein (*traD*) and a putative
202 relaxase of the MOB_F family (*traI*). Finally, two IMEs sharing an identical Sfx protein are
203 integrated at the 3' end of *tRNA-TRP* and the 5' end of *rlmD* in environmental isolates of
204 *Shewanella chilikensis* and *Shewanella putrefaciens*, respectively. Despite sharing a conserved
205 core set of genes with IE*Vch*Aut1, the Sfx protein of these two IMEs resembles and clusters
206 with Sfx_{94} (Fig 3A). Although we can predict AcaCD binding sites across these IMEs, they do
207 not share any other conserved features of the SGI1 and MGI*Vch*Hai6 families, suggesting they
208 belong to a novel unrelated IME family mobilizable by IncC plasmids.

209 **Surface exclusion specificity is determined by TraN**

210 To test the role of Sfx in the donor, we monitored the transfer of pClo from donors carrying the
211 Δ*eexC* and Δ*sfx* deletion mutants of $pVCR94^{Sp}$ toward an $IncC^+$ strain ($pVCR94^{Kn}$). No
212 alleviation of exclusion, i.e., an increase in transfer frequency, was observed (Fig 4A). On the
213 contrary, a modest yet significant decrease was observed for the Δ*eexC* Δ*sfx* mutant,
214 suggesting that augmented redundant transfer between donors was detrimental to transfer
215 toward recipients. Hence, *sfx* is not self-targeting to promote surface exclusion.
216 Next, we focused on TraN as a potential target for surface exclusion, as the gene *traN* encodes
217 a putative adhesin thought to stabilize the mating pair, and it is adjacent to *sfx* in most
218 conjugative plasmids found but pAQU1 [29,30,37]. A search for homologs of $TraN_{94}$ yielded 412
219 homologous proteins (S3 File), most encoded by ACL plasmids. Others belonged to IncC-
220 mobilizable IMEs of the SGI1 family integrated into *trmE* or *dusA*, with no clear relationship

221 between TraN phylogeny and insertion site (Fig 3B). The cluster represented by pAQU1 differs
222 significantly from the close ACL plasmids as the *dsbC-traC-trhF-traWUN* and *acaB*/*bet-exo*
223 regions are not adjacent, and *sfx* lies elsewhere.
224 To investigate the involvement of TraN in Sfx-dependent exclusion, we used in mating assays a
225 *traN* deletion mutant of pVCR94^{Sp} Δ*traN* complemented ectopically with either its native $traN_{94}$
226 or the distantly related homolog $traN_{AQU1}$ [38]. Whereas the expression of sfx_{94} in the recipient
227 strongly inhibited conjugation supported by $traN_{94}$, it did not impair transfer supported by
228 $traN_{AQU1}$ (Fig 4B). This result implies TraN is, if not a direct interactant of Sfx, a key player in
229 Sfx-mediated exclusion and the determinant of exclusion specificity. To further investigate the
230 diversity of exclusion specificity, we tested the *traN*/*sfx* pairs of pAsa4c and pAhD4-1, two
231 plasmids that belong to distinct entry exclusion groups, as well as pAQU1 [8,39,40]. The
232 corresponding genes were tested in pairs in all possible combinations to determine exclusion
233 indices. Two separate exclusion groups emerged (Fig 4C). *sfx* homologs from pVCR94, pAsa4c
234 and pAhD4-1 specifically exerted exclusion against *traN* homologs from these same plasmids.
235 sfx_{AQU1} only excluded $traN_{AQU1}$.

236 **Discussion**

237 All conjugative plasmids encode at least one exclusion factor [12]. An entry exclusion system
238 involving the entry exclusion factor EexC and the VirB6-homolog TraG was previously identified
239 in IncA and IncC conjugative plasmids [8]. Here, we identified a second exclusion factor within a
240 region suspected by Humbert *et al*. as responsible for additional exclusion activity [8]. A TraDIS
241 experiment pointed to nine candidate genes likely to enhance incoming transfer once disrupted.
242 *sfx* was the only one whose activity could be experimentally validated. Together, *eexC* and *sfx*
243 account for the totality of the exclusion phenotype (Fig 1D), akin to the exclusion mediated by
244 *traS* and *traT* of the F plasmid [41].

245 The translation product of *sfx* is a predicted lipoprotein. Here, we confirmed that Sfx is present
246 in the outer membrane (Fig 2B), a trait shared with the surface exclusion factor TraT of the F
247 plasmid and compatible with the proposed mechanism of surface exclusion [13,42]. We found
248 that *sfx* is constitutively expressed independently of AcaCD at a much higher level than *eexC*
249 (Fig 2DEF).
250 Our search in the Genbank database using Sfx_{94} failed to reveal any known entry or surface
251 exclusion factor, including F plasmid TraS or TraT, establishing Sfx as a novel surface exclusion
252 factor (S3 File). As pAsa4c and pAhD4-1 belong to the same surface exclusion group as
253 pVCR94 despite their divergence (Fig 4C), IncA and IncC plasmids are expected to exert
254 surface exclusion against each other, hence contributing alongside entry exclusion to the
255 previously observed exclusion phenotype between the two incompatibility groups [8,33]. Among
256 the Sfx homologs tested in this study, only Sfx_{AQU1}, which failed detection by the NCBI blastp
257 search due to low similarity with Sfx_{94}, belongs to a separate surface exclusion group (Fig 4C).
258 A pairwise comparison illustrates that similar to Sfx_{AQU1}, the putative surface exclusion proteins
259 WP_035235290.1 and WP_121638668.1 share minimal homology with all other representatives
260 (Fig 3A and S3 Fig). Therefore, we speculate that neither belongs to the two surface exclusion
261 groups described here and that all other IncC, IncA and close ACL plasmids belong to the Sfx_{94}
262 surface exclusion group. From our observations with ACL plasmids, surface exclusion strikingly
263 contrasts with entry exclusion, which seems much more specific. Indeed, pAsa4c and pAhD4-1
264 each belong to separate entry exclusion groups (EexE and EexD, respectively) distinct from the
265 one encompassing IncC and IncA plasmids (EexC); yet, all belong to the same surface
266 exclusion group [8]. These observations suggest IncC, IncA and ACL plasmids form a two-tier
267 community, exerting surface and entry exclusion against closely related peers but only surface
268 exclusion against a broader range of distantly related conjugative elements.

269 This work has also identified orphan surface exclusion factors borne by IMEs. IE*Ave*Tha1-like
270 elements belong to the MGI*Vch*Hai6 family of IncC-mobilizable IMEs [4,5], whereas IE*Vch*Aut1-
271 like elements constitute a new family of IMEs likely to be mobilizable by ACL plasmids (Fig 3C).
272 Since these IMEs lack a *traN* gene, we propose they engage in surface exclusion as a
273 defensive mechanism, forcing their host to favour mating partners that could enhance both their
274 stability and transmissibility. Hence, these IMEs could modulate the circulation of conjugative
275 elements in bacterial populations without affecting whether surface exclusion from a potential
276 recipient will target transfer mediated by their helper element. Such behaviour would contrast
277 with the way SGI1 manipulates the exclusion system of its helper IncC plasmid. SGI1, which is
278 not known to exert exclusion, evades IncC entry exclusion by substituting TraG in the mating
279 apparatus with a distant VirB6 homolog [10]. Manipulation of exclusion by mobilizable elements
280 is not well known. While homologous ColE1 mobilizable plasmids are known to inhibit each
281 other's transfer mildly, this phenotype was attributable to the accessory mob gene *mbeD* with no
282 identified target in the donor [19,43,44]. It thus remains unclear whether exclusion is at play in
283 that case. The putative IMEs we reported here may be the first instance of exclusion exerted by
284 mobilizable elements. The close relationship between Sfx proteins encoded by IE*Ave*Tha1 and
285 IE*Vch*Aut1 with those tested in this study (Sfx_{94}, Sfx_{AhD4-1}, and Sfx_{Asa4c}) suggests they belong to
286 the same exclusion group (Fig 3, S3 Fig). Should this activity be corroborated by experimental
287 evidence, it would establish exclusion as an actual barrier to the circulation of mobile genetic
288 elements on par with other bacterial defense mechanisms instead of being limited to preventing
289 redundant transfer and, potentially, mediating mating pair separation [12,37]. Surprisingly, none
290 of the IMEs identified by the TraN search, including SGI1, appears in the Sfx tree, suggesting
291 they do not encode a surface exclusion factor related to Sfx_{94}. Conversely, IMEs identified by
292 the Sfx search are ostensibly absent from the TraN tree as they lack the components of a

293 conjugative apparatus. This observation could indicate different survival strategies. Whereas
294 SGI1 maximizes its own dissemination by remodelling the mating apparatus to improve transfer
295 and bypass entry exclusion [10], IE*Ave*Tha1 and IE*Vch*Aut1 may ensure persistence by
296 hindering the entry of destabilizing, excision-inducing ACL plasmids via surface exclusion.
297 Although the mobilization mechanism of IE*Vch*Aut1 remains unknown, its gene content and the
298 presence of AcaCD binding motifs suggest mechanistic parallels with that of SGI1, albeit using
299 totally unrelated factors. In ACL^+ cells, AcaCD likely promotes IE*Vch*Aut1's excision through the
300 expression of *rdfM* [36]. A predicted homolog of the replication protein P from bacteriophage
301 lambda suggests the excised IME is replicative [45]. IME DNA transfer seems to rely on the
302 IME-encoded TraI, a predicted relaxase of the MOB_F family [46]. While SGI1 encodes its own
303 replication and DNA processing functions [9,47,48], IE*Vch*Aut1 additionally encodes a type IV
304 coupling protein, presumably making it independent from the IncC-encoded TraD and DtrJ (also
305 known as TraJ) [5,49].
306 IncHI1 EexB and IncF TraT are two other known surface exclusion factors. While EexB seems
307 to have a dual role as an exclusion factor and exclusion target, TraT's mechanism remains
308 elusive as exclusion specificity could not be attributed to direct interaction with pilin or indirect
309 interaction with the putative adhesin TraN through OmpA [14,26,27,29]. Our results
310 demonstrate that Sfx is only required in the recipient to enable exclusion (Fig 4A), ruling out the
311 self-targeting of Sfx. Instead, we found that Sfx exclusion can be neutralized by substituting
312 TraN in the donor with TraN from another surface exclusion group (Fig 4BC). Distinct exclusion
313 groups within a given family were previously reported in IncI and IncF plasmids and SXT/R391
314 ICEs [15,22,50–52].
315 Although a direct interaction between Eex and TraG has been suggested in SXT/R391 ICEs
316 and likely extends to other VirB6-targeting entry exclusion factors [25], direct contact between

317 Sfx and TraN is unlikely for surface exclusion. In fact, the binding of outer membrane proteins
318 on donor and recipient cells is hard to reconcile with the idea that surface exclusion physically
319 prevents the formation or disrupts mating aggregates [13].
320 Instead, surface exclusion factors have been proposed to act by concealing outer membrane
321 receptors involved in mating aggregation [28]. According to Riede and Eschbach, TraT of F
322 directly interacts with the major outer membrane protein OmpA as TraT inhibits the OmpA-
323 specific phage K3 [28]. Yet, despite ample evidence that $TraN_F$ interacts with OmpA during
324 conjugation, it does not seem to determine exclusion specificity as $TraN_F$ substitution with
325 $TraN_{R100-1}$ does not counter exclusion by TraT of F [29–31].
326 Our finding that *sfx* is expressed at a much higher level than *eexC* despite exerting a similar
327 level of exclusion (Fig 1D, Fig 2EF) is consistent with an interaction with a highly abundant
328 surface protein. While few EexC proteins might suffice to target TraG in one mating pore during
329 conjugation, an abundance of Sfx proteins is likely required to conceal most, if not all, TraN
330 receptors on the recipient surface at all times. Unlike TraT of F, we have identified TraN as the
331 specificity determinant for Sfx-mediated exclusion between ACL plasmids. Thus, we propose
332 that $TraN_{94}$ and $TraN_{AQU1}$ recognize distinct receptors on the recipient surface and that Sfx
333 prevents mating pair stabilization by specific binding to the receptor of its cognate TraN. Further
334 investigation will be required to identify the receptors involved.

336 ## Materials and methods

337 ### Bacterial strains and media

338 The bacterial strains and plasmids used in this study are described in Table 2. Bacterial strains
339 were grown at 37°C on Luria-Bertani (LB) agar or with agitation in LB broth and maintained at
340 −75°C in LB broth containing 20% (vol/vol) glycerol. Antibiotics were used at the following
341 concentrations: ampicillin (Ap), 100 µg/ml; kanamycin (Kn), 50 µg/ml; spectinomycin (Sp), 50
342 µg/ml; rifampicin (Rf), 50 µg/ml; chloramphenicol (Cm), 20 µg/ml and nalidixic acid (Nx), 40
343 µg/ml. Media were supplemented with 0.02% L-arabinose or 0.1 mM isopropyl β-D-1-
344 thiogalactopyranoside (IPTG) to induce gene expression from pBAD30 and pAH56 constructs,
345 respectively.

Table 2. Strains and plasmids used in this study

Strain, plasmid or element	Relevant genotype or phenotype	Reference
Escherichia coli		
GG56	Nx^r derivative of BW25113 (Nx)	[53]
KH95	Rf^r derivative of BW25113 (Rf)	[9]
MFD*pir*	MG1655 RP4-2-Tc::[ΔMu1::*aac(3)IV*-Δ*aphA*-Δ*nic35*-ΔMu2::*zeo*] Δ*dapA*::(*erm-pir*) Δ*recA*	[54]
VB112	Rf^r derivative of MG1655 (Rf)	[55]
CAG18439	MG1655 *lacZU118 lacI42*::Tn*10* (Tc)	[56]
Plasmids		
pVCR94	IncC conjugative plasmid, *V. cholerae* O1 El Tor (Su Tm Cm Ap Tc Sm)	[57]
$pVCR94^{Sp}$	Sp^r derivative of pVCR94 (pVCR94ΔX2) (Su Sp)	[10]
$pVCR94^{Kn}$	Kn^r derivative of pVCR94 (pVCR94ΔX3) (Su Kn)	[10]
$pVCR94^{Kn}$ Δ*eexC*::*cat*	*eex* deletion mutant of $pVCR94^{Kn}$ (Su Kn Cm)	This study
pFG036	ori_{pMB1}, *cI857* (Ts) repressor, *tetM* (Tc)	Addgene #137996
pFG051	ori_{R6K}, Tn*5 tnp* under λP_L promoter, $oriT_{RP4}$, Tn*5d-aadA7* (Sp)	Addgene #137997
$pVCR94^{Sp}$ Δ*018-019*	*vcrx018-vcrx019* deletion mutant of $pVCR94^{Sp}$ (Su Sp)	This study
$pVCR94^{Sp}$ Δ*062*	*vcrx062* deletion mutant of $pVCR94^{Sp}$ (Su Sp)	This study

pVCR94^{Sp} Δ*107-108*	*vcrx107-vcrx108* deletion mutant of pVCR94^{Sp} (Su Sp)	This study
pVCR94^{Sp} Δ*111*	*vcrx111* deletion mutant of pVCR94^{Sp} (Su Sp)	This study
pVCR94^{Sp} Δ*137*	*vcrx137* deletion mutant of pVCR94^{Sp} (Su Sp)	This study
pVCR94^{Sp} Δ*acr2*	*vcrx150* deletion mutant of pVCR94^{Sp} (Su Sp)	[6]
pVCR94^{Sp} Δ*eexC*	*vcrx145* deletion mutant of pVCR94^{Sp} (Su Sp)	[8]
pVCR94^{Sp} Δ*sfx*	*vcrx085* deletion mutant of pVCR94^{Sp} (Su Sp)	This study
pVCR94^{Sp} Δ*eexC*Δ*sfx*	*vcrx145-vcrx085* double deletion mutant of pVCR94^{Sp} (Su Sp Cm)	This study
pVCR94^{Kn} Δ*acaCD*	*acaCD* deletion mutant of pVCR94^{Kn} (Su Kn)	This study
pClo	CloDF13::TnAΔEcoRV (pSU4628) (Ap)	[58]
p*acaCD*	pBAD30::*acaCD* (Ap)	[6]
pVCR94^{Sp} Δ*traN*	*traN* deletion mutant of pVCR94^{Sp} (Su Sp)	[10]
pAsa4c	Cm^{r} conjugative plasmid from *A. salmonicida* JF2267 (Cm)	[39]
p*traN*$_{94}$	pBAD30::*traN*$_{pVCR94}$ (Ap)	[10]
p*traN*$_{Asa4c}$	pBAD30::*traN*$_{pAsa4c}$ (Ap)	This study
p*traN*$_{AhD4-1}$	pBAD30::*traN*$_{pAhD4-1}$ (Ap)	This study
p*traN*$_{AQU1}$	pBAD30::*traN*$_{pAQU1}$ (Ap)	This study
p*sfx*$_{94}$	pAH56::*sfx*$_{pVCR94}$ (Ap)	This study
p*sfx*$_{Asa4c}$	pAH56::*sfx*$_{pAsa4c}$ (Ap)	This study
p*sfx*$_{AhD4-1}$	pAH56::*sfx*$_{pAhD4-1}$ (Ap)	This study
p*sfx*$_{AQU1}$	pAH56::*sfx*$_{pAQU1}$ (Ap)	This study
p*eexC*	pAH56::*eex*$_{pVCR94}$ (Ap)	This study
p*sfx*$_{94}$-*3xFlag*	pAH56::*sfx*$_{pVCR94}$-*3xFlag* (Ap)	This study
pVCR94^{Kn} *eexC*'-'*lacZ*	Translational fusion of *lacZ* at the 8th codon of *vcrx145* (Su Kn)	This study
pVCR94^{Kn} *sfx*'-'*lacZ*	Translational fusion of *lacZ* at the 8th codon of *vcrx085* (Su Kn)	This study
pVCR94^{Kn} *eexC*'-'*lacZ* Δ*acaCD*	*acaCD* deletion mutant of pVCR94^{Kn} *eexC*'-'*lacZ* (Su Kn Cm)	This study
pVCR94^{Kn} *sfx*'-'*lacZ* Δ*acaCD*	*acaCD* deletion mutant of pVCR94^{Kn} *sfx*'-'*lacZ* (Su Kn Cm)	This study
pAH56	*ori*$V_{R6Kγ}$ *att*$P_{λ}$ *lacI* P_{tac} (Kn)	[59]
pBAD30	*ori*$_{p15A}$ *bla araC* P_{BAD} (Ap)	[60]
pINT-ts	*ori*$_{R101}$ *cI857* $λp_R$-*int*$_{λ}$ (ts, Ap)	[59]
pVI42b	pVI36 BamHI::P_{lac}-*lacZ* (Sp)	[61]
pKD3	*cat* template for one-step chromosomal gene inactivation (Cm)	[62]
pKD4	*aph* template for one-step chromosomal gene inactivation (Kn)	[62]
pCP20	Flp recombinase thermo-inducible encoding plasmid (ts, Ap Cm)	[63]
pSIM6	λ Red recombination thermo-inducible encoding plasmid (ts, Ap)	[64]

Ap, ampicillin; Cm, chloramphenicol; Kn, kanamycin; Nx, nalidixic acid; Rf, rifampicin; Sm, streptomycin; Sp, Spectinomycin; Su, sulfamethoxazole; Tc, tetracycline; Tm, trimethoprim; ts, thermosensitive

346

347 **Plasmids and strains construction**

348 Plasmid DNA was prepared using the QIAprep Spin Miniprep kit (Qiagen), and genomic DNA
349 was isolated with the QIAamp DNA mini kit (Qiagen) as recommended by the manufacturer.
350 PCR products were purified using the PCR purification kit (Qiagen). All molecular biology
351 manipulations were carried out by standard procedures following the Current Protocols in
352 Molecular Biology [65]. Transformation by electroporation was done using a Biorad Gene Pulser
353 Xcell apparatus (BioRad) in 1 mm cuvettes under the following conditions: 200 Ω, 25 µF and
354 either 18 kV/cm.
355 The oligonucleotides used in this study are described in Supplemental Table 1. Gene deletions
356 were constructed using the one-step chromosomal gene inactivation technique (λ Red-mediated
357 mutagenesis) with pKD3 and pKD4 as templates for antibiotic resistance cassettes [62].
358 The deletions of *vcrx018-vcrx019*, *vcrx062*, *vcrx085*, *vcrx107-vcrx108*, *vcrx111*, *vcrx137* and
359 *eexC* in pVCR94^{Sp} or pVCR94^{Kn} were done using primer pairs
360 94delvcrx018.for/94delvcrx019.rev, 94delvcrx062.for/94delvcrx062.rev,
361 94delvcrx085.for/94delvcrx085.rev, 94delvcrx107.for/94delvcrx108.rev,
362 94delvcrx111.for/94delvcrx111.rev, 94delvcrx137.for/94delvcrx137.rev and
363 94del145.for/94del145.rev, respectively, and pKD3 or pKD4 as the template. Deletion of
364 *vcrx085* in pVCR94^{Sp} Δ*eexC* was done using primer pair 94delsfx.for/94delsfx.rev and pKD3 as
365 the template. The λRed recombination system was expressed using pSIM6. When appropriate,
366 resistance cassettes were excised from the resulting constructions using the Flp-encoding
367 plasmids pCP20. All deletions were validated by antibiotic profiling and PCR.

368 The *eexC'-'lacZ* and *sfx'-'lacZ* fusions were introduced into pVCR94^{Kn} using primer pairs 94eex-
369 lacZ.f/94eex-lacZ.r and 94sfx-lacZ.f/94sfx-lacZ.r and pVI42b as the template. The deletion of
370 *acaCD* in pVCR94^{Kn}, pVCR94^{Kn} *eexC'-'lacZ* and pVCR94^{Kn} *sfx'-'lacZ* was done using primer
371 pair 94DelacaD.for/94DelacaC.rev and pKD3 as the template.
372 pVCR94 and pAsa4c served as templates to amplify their respective genes of interest. $sfx_{AhD4\text{-}1}$,
373 sfx_{AQU1}, $traN_{AhD4\text{-}1}$ and $traN_{AQU1}$ were chemically synthesized and obtained from Bio Basic.
374 sfx_{94}, sfx_{Asa4c}, $sfx_{AhD4\text{-}1}$, sfx_{AQU1} and *eexC* were amplified using primer pairs
375 94sfxNdeI.f/94sfxSalI.r, Asa4sfxNdeI.f/Asa4sfxSalI.r, AhD4sfxNdeI.f/AhD4sfxSalI.r,
376 AQU1sfxNdeI.f/AQU1sfxSalI.r and eexCNdeI.f/eexCSalI.r, respectively. Amplicons were
377 digested with NdeI and SalI and cloned into NdeI/SalI-digested pAH56. psfx_{94}-*3xFlag* was
378 constructed from psfx_{94} using primer pair pAH56_3xFlag.F/94sfx_3xFlag.R and the Q5 Site-
379 Directed Mutagenesis Kit (New England Biolabs) according to the manufacturer's instructions.
380 The resulting constructs were single-copy integrated into the $attB_{\lambda}$ chromosomal site of
381 BW25113 using pINT-ts.
382 $traN_{Asa4c}$, $traN_{AhD4\text{-}1}$, $traN_{AQU1}$ were amplified using primer pairs Asa4traNEcoRI.f/Asa4traNSalI.r,
383 AhD4traNEcoRI.for/AhD4traNEcoRI.rev and AQU1traNEcoRI.for/AQU1traNEcoRI.rev,
384 respectively. Amplicons were digested with EcoRI or EcoRI/SalI and cloned into EcoRI- or
385 EcoRI/SalI-digested pBAD30.
386 All constructs were verified by PCR and DNA sequencing at the Plateforme de Séquençage et
387 de Génotypage du Centre de Recherche du CHUL (Québec, QC, Canada).

388 **Conjugation assays**

389 Bacteria were grown for 16 h in LB broth with the appropriate antibiotics. Mating assays were
390 carried out by mixing 100 µl of donor and recipient cells. Cells were pelleted by centrifugation,
391 then washed once in 1 volume of LB broth and resuspended in 1/20 volume of LB broth.

392 Bacterial mixtures were incubated for 6 h on LB agar plates at 37°C to allow conjugation. Serial
393 dilutions were then plated on selective LB-agar plates with appropriate antibiotics to discriminate
394 between donor, recipient and transconjugant CFUs. Transfer frequencies were calculated by
395 dividing the number of transconjugant CFUs by the number of donor CFUs. Exclusion indices
396 were calculated as the ratio of an element's transfer frequency toward an empty recipient to its
397 transfer frequency toward the tested recipient.

398 **Transposon-directed insertion sequencing (TraDIS)**

399 A conjugation-assisted random transposon mutagenesis experiment was performed on *E. coli*
400 GG56 bearing pVCR94^{Kn} Δ*eexC*::*cat*. The transposition system was composed of *E. coli*
401 MFD*pir* carrying pFG036 (a plasmid coding for a thermosensitive cI transcriptional repressor)
402 and pFG051 (a Pi-dependent RP4-mobilizable plasmid coding for the Tn*5* transposition
403 machinery repressed by cI, and carrying a mini-Tn*5* (Sp) transposon). This diaminopimelate
404 (DAP)-auxotrophic strain contains a chromosomal RP4 conjugative machinery and expresses
405 the Pi protein required for pFG051 replication. The TnSeq experiment was performed in several
406 successive steps. First, pFG051 was transferred by conjugation from MFD*pir* to GG56 bearing
407 pVCR94^{Kn} Δ*eexC*::*cat* in a 2-h mating experiment at 30°C on LB agar plates supplemented with
408 DAP in duplicates. Once in the recipient strain that lacks cI, the constitutively expressed Tn*5*
409 machinery of pFG051 mediates random mini-Tn*5* (Sp) insertions in the genome. The mating
410 mixture was then entirely spread onto 40 large LB agar plates (150 mm) supplemented with Cm,
411 Kn, Nx, and Sp. Plates were incubated until near confluence (40k to 60k CFUs) to select clones
412 carrying mini-Tn*5* (Sp) insertions. After overnight incubation at 37°C, Cm Nx Kn Sp-resistant
413 colonies were collected using a cell scraper and resuspended in LB broth. The collected
414 sample, designated as the 'input library' was washed, then resuspended in 4.5 ml of LB broth
415 and cryopreserved. The total DNA of a 1.5 ml aliquot of the input library was extracted for

416 sequencing. Another 1 ml aliquot of input library was used to inoculate 50 ml of LB broth
417 supplemented with Cm, Kn, Nx and Sp, which was then grown overnight at 37°C. The resulting
418 culture was used as the recipient in a mating assay, mixed in equal volumes with *E. coli* KH95
419 carrying pVCR94^{Kn} and pClo. After a 2-h incubation at 37°C, mating mixtures were spread onto
420 20 large LB agar plates (150 mm) supplemented with Nx, Kn, Sp, Cm, and Ap to select for mini-
421 Tn*5* (Sp) insertions in pVCR94^{Kn} Δ*eexC*::*cat* that allowed transmission and replication of pClo
422 into the recipients. After overnight incubation at 37°C, Nx, Kn, Sp, Cm, and Ap-resistant
423 colonies were collected and subsequently resuspended in LB broth, washed and resuspended
424 in 4.5 ml of LB broth and cryopreserved. These samples were designated as 'output libraries'.
425 The total DNA of a 1.5 ml aliquot of the output libraries was extracted and used for sequencing.

426 **Preparation of TnSeq libraries and Illumina sequencing**

427 For each library, a 1.5 ml frozen stock aliquot was thawed on ice for 15 minutes and used to
428 prepare sequencing libraries as described previously [66]. Mutant libraries were then pooled
429 and sequenced by Illumina using the NextSeq® 500/550 High Output Kit v2 at the RNomics
430 platform of the Laboratoire de Génomique Fonctionnelle de l'Université de Sherbrooke
431 (https://rnomics.med.usherbrooke.ca) (Sherbrooke, QC, Canada). The transposon data analysis
432 was carried out as described previously [66].

433 **Protein purification and analysis**

434 *E. coli* BL21 containing a single-copy, chromosomally integrated p*sfx*$_{94}$-*3xFlag* was grown to an
435 OD_{600} = 0.8 in the presence of 0.1 mM IPTG. Cells were subjected to a lysozyme/EDTA lysis
436 followed by selective detergent treatment to isolate the outer membrane fraction [67]. The lysate
437 (total cell extract) and the pellet containing the outer membrane fraction (final volume: 225 µl)
438 resuspended in NuPAGE LDS Sample Buffer (Invitrogen) and supplemented with NuPAGE

439 Sample Reducing agent (Invitrogen) were incubated at 70°C for 10 min before loading on a 12%
440 SDS-PAGE gel. Proteins were then either stained with Coomassie brilliant blue R-250 (Bio-Rad)
441 or transferred onto a polyvinylidene fluoride (PVDF) membrane. Western blotting was performed
442 according to standard procedures. Sfx_{94}-3xFLAG was detected using a rabbit anti-FLAG primary
443 antibody (Sigma-Aldrich, cat. # F7425) and an HRP goat anti-rabbit IgG HRP-conjugated
444 secondary antibody (Invitrogen, cat. # G-21234).

445 **Molecular biology**

446 Plasmid DNA was extracted using the EZ-10 Spin Column Plasmid DNA Minipreps Kit (Bio
447 Basic) following the manufacturer's instructions. Enzymes used in this study were purchased
448 from New England Biolabs. PCR assays were performed with primers listed in Table S1. PCR
449 conditions were as follows: (i) 3 min at 94°C; (ii) 30 cycles of 30 s at 94°C, 30 s at the
450 appropriate annealing temperature, and 1 minute/kb at 68°C; and (iii) 5 min at 68°C. When
451 required, the resulting products were purified using the EZ-10 Spin Column PCR Products
452 Purification Kit (Bio Basic) following the manufacturer's instructions. E. coli strains were
453 transformed by electroporation as described previously [68] in a Bio-Rad Gene Pulser Xcell
454 device set at 25 µF, 200 V and 1.8 kV using 1-mm gap electroporation cuvettes.

455 **RNA extraction and cDNA synthesis**

456 RNA extractions were performed as follows. *E. coli* GG56 containing $pVCR94^{Kn}$ with or without
457 p*acaCD* was grown at 37°C for 16 h in LB broth containing the appropriate antibiotics. The
458 cultures were diluted 1:200 in fresh medium containing the appropriate antibiotics and grown to
459 an OD_{600} of 0.2 before being diluted 1:10 again in fresh medium containing the appropriate
460 antibiotics and supplemented with 0.02% arabinose when needed. After a 2-h incubation period,
461 4 ml of the cultures were used for total RNA extraction using the Direct-zol RNA extraction kit

462 (Zymo Research) and TRI Reagent (Sigma-Aldrich) according to the manufacturer's
463 instructions. Once purified, the RNA samples were treated using 2 units of DNase I (New
464 England Biolabs) according to the manufacturer's instructions to eliminate residual gDNA. cDNA
465 was synthesized from 0.5 ng of RNA and 1 pmol of gene-specific primer 85RT (Integrated DNA
466 Technologies) using the reverse transcriptase SuperScript IV (Invitrogen), according to the
467 manufacturer's instructions. Control reactions without reverse transcriptase treatment ('RNA')
468 were performed for each sample. PCR reactions aiming at amplifying sfx_{94} and *acaD* were
469 carried out using 50 pg of RNA or the corresponding amount of cDNA, or 0.5 ng of gDNA as the
470 template, and primer pairs sfxF/sfxR and 086F2/086R2, respectively.

471 **β-galactosidase assays**

472 Qualitative assays were performed by depositing 10 µl aliquots of overnight cultures with
473 appropriate antibiotics on solid agar supplemented with 5-bromo-4-chloro-3-indolyl-β-D-
474 galactopyranoside (X-gal) with or without 0.02% arabinose. The plates were observed after
475 overnight incubation at 37°C.
476 Quantitative assays were performed with 2-nitrophenyl-β-D-galactopyranoside (ONPG)
477 according to a protocol adapted from Miller [69]. After overnight incubation at 37°C with
478 appropriate antibiotics, cultures were diluted 1:100 in 50ml LB broth supplemented with 50
479 µg/ml ampicillin and grown until an OD_{600} of 0.2 was reached. Three series of 1/10 dilutions
480 were then prepared in total volumes of 5 ml LB broth supplemented with 50 µg/ml ampicillin with
481 or without 0.2% arabinose and incubated for 2 hours at 37°C.

482 **Statistical analyses for conjugation assays**

483 Numerical data presented in graphs are available in S3 Dataset. All analyses were performed
484 using R Statistical Software (v4.2.1) and RStudio (v2022.12.0.252) [70]. We assumed a normal

485 distribution of the frequencies of transconjugant formation and tested the homogeneity of
486 variance of the log10-transformed frequencies using Bartlett's tests. Dunnett and Tukey-Kramer
487 tests and compact letter display were performed via the multcomp R package (v1.4-20) [71].
488 Details regarding statistical tests are provided in S2 File. Graphics were rendered via the
489 ggplot2 R package (v3.3.6) [72]. All figures were prepared using Inkscape 0.92
490 (https://inkscape.org/).

491 **Phylogenetic analyses**

492 The primary sequence of homologs of Sfx_{94} and $TraN_{94}$ were obtained using the NCBI blastp
493 algorithm [73] against the nr/nt database restricted to Gammaproteobacteria (taxid: 1236).
494 Primary sequences sharing less than 45% identity and under 85% minimum coverage were
495 filtered out of subsequent analyses. The distantly related Sfx_{AQU1} from pAQU1 was added
496 manually to the Sfx dataset as an outgroup. The datasets were clustered with CD-HIT [74] to
497 the best cluster that met the 0.90 identity cut-off before alignment. Where applicable,
498 representative sequences ("seeds") were manually substituted with sequences of interest within
499 the same clusters for downstream analyses. The resulting datasets were then aligned with
500 MUSCLE [75], and poorly aligned regions were discarded from the resulting amino acid
501 alignments using TrimAl v1.3 software with the automated heuristic approach [76]. Evolutionary
502 analyses were performed within MEGA11 (v 11.0.13) [77] using the Maximum Likelihood
503 method (PhyML) [78] and the Le and Gascuel matrix-based model [79] with gamma distribution
504 (LG + G). Initial tree(s) for the heuristic search were obtained automatically by applying
505 Neighbor-Join and BioNJ algorithms to a matrix of pairwise distances estimated using a JTT
506 model and then selecting the topology with superior log likelihood value. Percent identity values
507 were retrieved from the MUSCLE output [75].

508 **Bioinformatic predictions**

509 The prediction of signal peptides and cleavage sites in Sfx_{94} and $TraN_{94}$ was performed using
510 SignalP 6.0 with the slow model mode against other organisms [80]. Terminators were predicted
511 on both strands using ARNold [81,82]. *oriT* loci and mobilization proteins in putative IMEs were
512 predicted by oriTfinder [83].

513 **Data availability**

514 Raw sequencing data of TraDIS experiments were submitted to Genbank Sequence Read
515 Archive (SRA) under BioProject accession number PRJNA857050 with the following BioSample
516 accession numbers: SAMN32907975 and SAMN32907976 for *E. coli* BW25113 Nx bearing
517 pVCR94^{Kn} Δ*eexC*::*cat* as the recipient strain (input); SAMN32907978 and SAMN32907979 for
518 *E. coli* BW25113 Nx transconjugants bearing pVCR94^{Kn} Δ*eexC*::*cat* and pSU4628 (output).
519 Complete data from aligned reads can also be visualized using the UCSC genome browser [84]
520 at https://genome.ucsc.edu/cgi-
521 bin/hgHubConnect?hgHub_do_redirect=on&hgHubConnect.remakeTrackHub=on&hgHub_do_fi
522 rstDb=1&hubUrl=https://datahub-101-cw2.p.genap.ca/Rivard_2023/pVCR94dX3deexC.hub.txt.
523
524

525 **Acknowledgement**

526 We are grateful to Emilie Boulerne, Colin Poirier, Simon Jeanneau, and Frédéric Grenier for
527 technical assistance.

528 **References**

529 1. Harmer CJ, Hall RM. The A to Z of A/C plasmids. Plasmid. 2015;80: 63–82.
530 doi:10.1016/j.plasmid.2015.04.003

531 2. Doublet B, Boyd D, Mulvey MR, Cloeckaert A. The *Salmonella* genomic island 1 is an
532 integrative mobilizable element. Molecular Microbiology. 2005;55: 1911–1924.
533 doi:10.1111/j.1365-2958.2005.04520.x

534 3. Douard G, Praud K, Cloeckaert A, Doublet B. The *Salmonella* Genomic Island 1 Is
535 Specifically Mobilized *In Trans* by the IncA/C Multidrug Resistance Plasmid Family. PLoS
536 One. 2010;5. doi:10.1371/journal.pone.0015302

537 4. Carraro N, Rivard N, Ceccarelli D, Colwell RR, Burrus V. IncA/C Conjugative Plasmids
538 Mobilize a New Family of Multidrug Resistance Islands in Clinical *Vibrio cholerae* Non-
539 O1/Non-O139 Isolates from Haiti. mBio. 2016;7: e00509-16. doi:10.1128/mBio.00509-16

540 5. Rivard N, Colwell RR, Burrus V. Antibiotic Resistance in *Vibrio cholerae*: Mechanistic
541 Insights from IncC Plasmid-Mediated Dissemination of a Novel Family of Genomic Islands
542 Inserted at *trmE*. mSphere. 2020;5. doi:10.1128/mSphere.00748-20

543 6. Carraro N, Matteau D, Luo P, Rodrigue S, Burrus V. The Master Activator of IncA/C
544 Conjugative Plasmids Stimulates Genomic Islands and Multidrug Resistance Dissemination.
545 PLoS Genet. 2014;10. doi:10.1371/journal.pgen.1004714

546 7. Poulin-Laprade D, Carraro N, Burrus V. The extended regulatory networks of SXT/R391
547 integrative and conjugative elements and IncA/C conjugative plasmids. Front Microbiol.
548 2015;6. doi:10.3389/fmicb.2015.00837

549 8. Humbert M, Huguet KT, Coulombe F, Burrus V. Entry Exclusion of Conjugative Plasmids of
550 the IncA, IncC, and Related Untyped Incompatibility Groups. J Bacteriol. 2019;201: e00731-
551 18. doi:10.1128/JB.00731-18

552 9. Huguet KT, Rivard N, Garneau D, Palanee J, Burrus V. Replication of the *Salmonella*
553 Genomic Island 1 (SGI1) triggered by helper IncC conjugative plasmids promotes
554 incompatibility and plasmid loss. PLoS Genet. 2020;16. doi:10.1371/journal.pgen.1008965

555 10. Carraro N, Durand R, Rivard N, Anquetil C, Barrette C, Humbert M, et al. *Salmonella*
556 genomic island 1 (SGI1) reshapes the mating apparatus of IncC conjugative plasmids to
557 promote self-propagation. PLoS Genet. 2017;13. doi:10.1371/journal.pgen.1006705

558 11. Novick RP. Plasmid incompatibility. Microbiol Rev. 1987;51: 381–395.

559 12. Garcillán-Barcia MP, de la Cruz F. Why is entry exclusion an essential feature of
560 conjugative plasmids? Plasmid. 2008;60: 1–18. doi:10.1016/j.plasmid.2008.03.002

561 13. Achtman M, Kennedy N, Skurray R. Cell-cell interactions in conjugating *Escherichia coli*:
562 role of *traT* protein in surface exclusion. Proc Natl Acad Sci U S A. 1977;74: 5104–5108.

563 14. Gunton JE, Ussher JER, Rooker MM, Wetsch NM, Alonso G, Taylor DE. Entry exclusion in
564 the IncHI1 plasmid R27 is mediated by EexA and EexB. Plasmid. 2008;59: 86–101.
565 doi:10.1016/j.plasmid.2007.11.004

566 15. Sakuma T, Tazumi S, Furuya N, Komano T. ExcA proteins of IncI1 plasmid R64 and IncIγ
567 plasmid R621a recognize different segments of their cognate TraY proteins in entry
568 exclusion. Plasmid. 2013;69: 138–145. doi:10.1016/j.plasmid.2012.11.004

569 16. Pohlman RF, Genetti HD, Winans SC. Entry Exclusion of the IncN Plasmid pKM101 Is
570 Mediated by a Single Hydrophilic Protein Containing a Lipid Attachment Motif. Plasmid.
571 1994;31: 158–165. doi:10.1006/plas.1994.1017

572 17. Haase J, Kalkum M, Lanka E. TrbK, a small cytoplasmic membrane lipoprotein, functions in
573 entry exclusion of the IncP alpha plasmid RP4. J Bacteriol. 1996;178: 6720–6729.

574 18. Bolland S, Llosa M, Avila P, de la Cruz F. General organization of the conjugal transfer
575 genes of the IncW plasmid R388 and interactions between R388 and IncN and IncP
576 plasmids. J Bacteriol. 1990;172: 5795–5802.

577 19. Yamada Y, Yamada M, Nakazawa A. A ColE1-encoded gene directs entry exclusion of the
578 plasmid. J Bacteriol. 1995;177: 6064–6068.

579 20. Kamruzzaman M, Mathers AJ, Iredell JR. A Novel Plasmid Entry Exclusion System in
580 pKPC_UVA01, a Promiscuous Conjugative Plasmid Carrying the bla_{KPC} Carbapenemase
581 Gene. Antimicrob Agents Chemother. 66: e02322-21. doi:10.1128/aac.02322-21

582 21. Schmitt A, Hirt H, Järvå MA, Sun W-S, ter Beek J, Dunny GM, et al. Enterococcal PrgA
583 Extends Far Outside the Cell and Provides Surface Exclusion to Protect against Unwanted
584 Conjugation. Journal of Molecular Biology. 2020;432: 5681–5695.
585 doi:10.1016/j.jmb.2020.08.018

586 22. Marrero J, Waldor MK. The SXT/R391 Family of Integrative Conjugative Elements Is
587 Composed of Two Exclusion Groups. J Bacteriol. 2007;189: 3302–3305.
588 doi:10.1128/JB.01902-06

589 23. Avello M, Davis KP, Grossman AD. Identification, characterization, and benefits of an
590 exclusion system in an integrative and conjugative element of *Bacillus subtilis*. Mol
591 Microbiol. 2019;112: 1066–1082. doi:10.1111/mmi.14359

592 24. Meynell E, Ewins A. Effect on Exclusion of Alterations to the Sex Pilus. J Bacteriol.
593 1973;113: 71–75.

594 25. Marrero J, Waldor MK. Determinants of Entry Exclusion within Eex and TraG Are
595 Cytoplasmic. J Bacteriol. 2007;189: 6469–6473. doi:10.1128/JB.00522-07

596 26. Harrison JL, Taylor IM, Platt K, O'Connor CD. Surface exclusion specificity of the TraT
597 lipoprotein is determined by single alterations in a five-amino-acid region of the protein.
598 Molecular Microbiology. 1992;6: 2825–2832. doi:10.1111/j.1365-2958.1992.tb01462.x

27. Anthony KG, Sherburne C, Sherburne R, Frost LS. The role of the pilus in recipient cell recognition during bacterial conjugation mediated by F-like plasmids. Molecular Microbiology. 1994;13: 939–953. doi:10.1111/j.1365-2958.1994.tb00486.x

28. Riede I, Eschbach M-L. Evidence that TraT interacts with OmpA of *Escherichia coli*. FEBS Letters. 1986;205: 241–245. doi:10.1016/0014-5793(86)80905-X

29. Klimke WA, Frost LS. Genetic Analysis of the Role of the Transfer Gene, *traN*, of the F and R100-1 Plasmids in Mating Pair Stabilization during Conjugation. J Bacteriol. 1998;180: 4036–4043.

30. Klimke WA, Rypien CD, Klinger B, Kennedy RA, Rodriguez-Maillard JM, Frost LS. The mating pair stabilization protein, TraN, of the F plasmid is an outer-membrane protein with two regions that are important for its function in conjugation. Microbiology. 2005;151: 3527–3540. doi:10.1099/mic.0.28025-0

31. Low WW, Wong JLC, Beltran LC, Seddon C, David S, Kwong H-S, et al. Mating pair stabilization mediates bacterial conjugation species specificity. Nat Microbiol. 2022;7: 1016–1027. doi:10.1038/s41564-022-01146-4

32. Low WW, Seddon C, Beis K, Frankel G. The Interaction of the F-Like Plasmid-Encoded TraN Isoforms with Their Cognate Outer Membrane Receptors. Journal of Bacteriology. 2023;205: e00061-23. doi:10.1128/jb.00061-23

33. Ambrose SJ, Harmer CJ, Hall RM. Compatibility and entry exclusion of IncA and IncC plasmids revisited: IncA and IncC plasmids are compatible. Plasmid. doi:10.1016/j.plasmid.2018.02.002

34. Nivaskumar M, Francetic O. Type II secretion system: A magic beanstalk or a protein escalator. Biochimica et Biophysica Acta (BBA) - Molecular Cell Research. 2014;1843: 1568–1577. doi:10.1016/j.bbamcr.2013.12.020

35. Hancock SJ, Phan M-D, Luo Z, Lo AW, Peters KM, Nhu NTK, et al. Comprehensive analysis of IncC plasmid conjugation identifies a crucial role for the transcriptional regulator AcaB. Nature Microbiology. 2020; 1–9. doi:10.1038/s41564-020-0775-0

36. Daccord A, Mursell M, Poulin-Laprade D, Burrus V. Dynamics of the SetCD-Regulated Integration and Excision of Genomic Islands Mobilized by Integrating Conjugative Elements of the SXT/R391 Family. J Bacteriol. 2012;194: 5794–5802. doi:10.1128/JB.01093-12

37. Lawley TD, Klimke WA, Gubbins MJ, Frost LS. F factor conjugation is a true type IV secretion system. FEMS Microbiology Letters. 2003;224: 1–15. doi:10.1016/S0378-1097(03)00430-0

38. Nonaka L, Maruyama F, Miyamoto M, Miyakoshi M, Kurokawa K, Masuda M. Novel Conjugative Transferable Multiple Drug Resistance Plasmid pAQU1 from *Photobacterium damselae* subsp. *damselae* Isolated from Marine Aquaculture Environment. Microbes Environ. 2012;27: 263–272. doi:10.1264/jsme2.ME11338

636 39. Tanaka KH, Vincent AT, Trudel MV, Paquet VE, Frenette M, Charette SJ. The mosaic
637 architecture of *Aeromonas salmonicida* subsp. *salmonicida* pAsa4 plasmid and its
638 consequences on antibiotic resistance. PeerJ. 2016;4: e2595. doi:10.7717/peerj.2595

639 40. Zhu L, Zheng J-S, Wang W-M, Luo Y. Complete Genome Sequence of Highly Virulent
640 *Aeromonas hydrophila* Strain D4, Isolated from a Diseased Blunt-Snout Bream in China.
641 Microbiol Resour Announc. 2019;8: e01035-18. doi:10.1128/MRA.01035-18

642 41. Achtman M, Manning PA, Kusecek B, Schwuchow S, Neil W. Genetic analysis of F sex
643 factor cistrons needed for surface exclusion in *Escherichia coli*. Journal of Molecular
644 Biology. 1980;138: 779–795. doi:10.1016/0022-2836(80)90065-0

645 42. Perumal NB, Minkley EG. The product of the F sex factor *traT* surface exclusion gene is a
646 lipoprotein. Journal of Biological Chemistry. 1984;259: 5357–5360. doi:10.1016/S0021-
647 9258(18)91011-2

648 43. Inselburg J. Incompatibility Exhibited by Colicin Plasmids E1, E2, and E3 in *Escherichia coli*.
649 J Bacteriol. 1974;119: 478–483.

650 44. Chan PT, Ohmori H, Tomizawa J, Lebowitz J. Nucleotide sequence and gene organization
651 of ColE1 DNA. Journal of Biological Chemistry. 1985;260: 8925–8935. doi:10.1016/S0021-
652 9258(17)39438-3

653 45. Friedman DI, Olson ER, Georgopoulos C, Tilly K, Herskowitz I, Banuett F. Interactions of
654 bacteriophage and host macromolecules in the growth of bacteriophage lambda. Microbiol
655 Rev. 1984;48: 299–325.

656 46. Garcillán-Barcia MP, Francia MV, De La Cruz F. The diversity of conjugative relaxases and
657 its application in plasmid classification. FEMS Microbiology Reviews. 2009;33: 657–687.
658 doi:10.1111/j.1574-6976.2009.00168.x

659 47. Szabó M, Murányi G, Kiss J. IncC helper dependent plasmid-like replication of *Salmonella*
660 Genomic Island 1. Nucleic Acids Res. 2021;49: 832–846. doi:10.1093/nar/gkaa1257

661 48. Kiss J, Szabó M, Hegyi A, Douard G, Praud K, Nagy I, et al. Identification and
662 Characterization of *oriT* and Two Mobilization Genes Required for Conjugative Transfer of
663 *Salmonella* Genomic Island 1. Front Microbiol. 2019;10. doi:10.3389/fmicb.2019.00457

664 49. Hancock SJ, Phan M-D, Roberts LW, Vu TNM, Harris PNA, Beatson SA, et al.
665 Characterization of DtrJ as an IncC plasmid conjugative DNA transfer component. Molecular
666 Microbiology. 2021;116: 154–167. doi:https://doi.org/10.1111/mmi.14697

667 50. Hedges RW, Datta N. Plasmids Determining I Pili Constitute a Compatibility Complex.
668 Microbiology. 1973;77: 19–25. doi:10.1099/00221287-77-1-19

669 51. Willetts N, Maule J. Interactions between the surface exclusion systems of some F-like
670 plasmids. Genetics Research. 1974;24: 81–89. doi:10.1017/S0016672300015093

671 52. Willetts N, Maule J. Specificities of IncF plasmid conjugation genes. Genet Res. 1986;47: 1–
672 11. doi:10.1017/s0016672300024447

673 53. Grenier F, Matteau D, Baby V, Rodrigue S. Complete Genome Sequence of *Escherichia coli*
674 BW25113. Genome Announc. 2014;2: e01038-14. doi:10.1128/genomeA.01038-14

675 54. Ferrières L, Hémery G, Nham T, Guérout A-M, Mazel D, Beloin C, et al. Silent Mischief:
676 Bacteriophage Mu Insertions Contaminate Products of Escherichia coli Random
677 Mutagenesis Performed Using Suicidal Transposon Delivery Plasmids Mobilized by Broad-
678 Host-Range RP4 Conjugative Machinery. J Bacteriol. 2010;192: 6418–6427.
679 doi:10.1128/JB.00621-10

680 55. Ceccarelli D, Daccord A, René M, Burrus V. Identification of the Origin of Transfer (*oriT*) and
681 a New Gene Required for Mobilization of the SXT/R391 Family of Integrating Conjugative
682 Elements. J Bacteriol. 2008;190: 5328–5338. doi:10.1128/JB.00150-08

683 56. Singer M, Baker TA, Schnitzler G, Deischel SM, Goel M, Dove W, et al. A collection of
684 strains containing genetically linked alternating antibiotic resistance elements for genetic
685 mapping of *Escherichia coli*. Microbiol Rev. 1989;53: 1–24.

686 57. Carraro N, Sauvé M, Matteau D, Lauzon G, Rodrigue S, Burrus V. Development of
687 pVCR94ΔX from *Vibrio cholerae*, a prototype for studying multidrug resistant IncA/C
688 conjugative plasmids. Front Microbiol. 2014;5. doi:10.3389/fmicb.2014.00044

689 58. Cabezón E, Sastre JI, de la Cruz F. Genetic evidence of a coupling role for the TraG protein
690 family in bacterial conjugation. Mol Gen Genet. 1997;254: 400–406.

691 59. Haldimann A, Wanner BL. Conditional-Replication, Integration, Excision, and Retrieval
692 Plasmid-Host Systems for Gene Structure-Function Studies of Bacteria. J Bacteriol.
693 2001;183: 6384–6393. doi:10.1128/JB.183.21.6384-6393.2001

694 60. Guzman LM, Belin D, Carson MJ, Beckwith J. Tight regulation, modulation, and high-level
695 expression by vectors containing the arabinose P_{BAD} promoter. Journal of Bacteriology.
696 1995;177: 4121–4130. doi:10.1128/jb.177.14.4121-4130.1995

697 61. Garriss G, Waldor MK, Burrus V. Mobile Antibiotic Resistance Encoding Elements Promote
698 Their Own Diversity. PLoS Genet. 2009;5. doi:10.1371/journal.pgen.1000775

699 62. Datsenko KA, Wanner BL. One-step inactivation of chromosomal genes in *Escherichia coli*
700 K-12 using PCR products. Proc Natl Acad Sci U S A. 2000;97: 6640–6645.

701 63. Cherepanov PP, Wackernagel W. Gene disruption in *Escherichia coli*: Tc^R and Km^R
702 cassettes with the option of Flp-catalyzed excision of the antibiotic-resistance determinant.
703 Gene. 1995;158: 9–14. doi:10.1016/0378-1119(95)00193-A

704 64. Datta S, Costantino N, Court DL. A set of recombineering plasmids for gram-negative
705 bacteria. Gene. 2006;379: 109–115. doi:10.1016/j.gene.2006.04.018

706 65. Ausubel FM, Brent R, Kingston RE, Moore DD, Seidman JG, Smith JA, et al. Current
707 Protocols in Molecular Biology. Hoboken: John Wiley & Sons; 2003.

708 66. Roy D, Huguet KT, Grenier F, Burrus V. IncC conjugative plasmids and SXT/R391 elements
709 repair double-strand breaks caused by CRISPR-Cas during conjugation. Nucleic Acids Res.
710 2020;48: 8815–8827. doi:10.1093/nar/gkaa518

711 67. Thein M, Sauer G, Paramasivam N, Grin I, Linke D. Efficient Subfractionation of Gram-
712 Negative Bacteria for Proteomics Studies. J Proteome Res. 2010;9: 6135–6147.
713 doi:10.1021/pr1002438

714 68. Dower WJ, Miller JF, Ragsdale CW. High efficiency transformation of *E. coli* by high voltage
715 electroporation. Nucleic Acids Res. 1988;16: 6127–6145. doi:10.1093/nar/16.13.6127

716 69. Miller JF. A short course in bacterial genetics. Plainview, NY: Cold Spring Harbor Laboratory
717 Press; 1992.

718 70. R Core Team. R: A Language and Environment for Statistical Computing. Vienna, Austria: R
719 Foundation for Statistical Computing; 2021. Available: https://www.R-project.org/

720 71. Hothorn T, Bretz F, Westfall P. Simultaneous inference in general parametric models. Biom
721 J. 2008;50: 346–363. doi:10.1002/bimj.200810425

722 72. Wickham H. ggplot2: Elegant Graphics for Data Analysis. New York, NY: Springer-Verlag;
723 2016.

724 73. Altschul SF, Gish W, Miller W, Myers EW, Lipman DJ. Basic local alignment search tool. J
725 Mol Biol. 1990;215: 403–410. doi:10.1016/S0022-2836(05)80360-2

726 74. Li W, Godzik A. Cd-hit: a fast program for clustering and comparing large sets of protein or
727 nucleotide sequences. Bioinformatics. 2006;22: 1658–1659.
728 doi:10.1093/bioinformatics/btl158

729 75. Edgar RC. MUSCLE: multiple sequence alignment with high accuracy and high throughput.
730 Nucleic Acids Res. 2004;32: 1792–1797. doi:10.1093/nar/gkh340

731 76. Capella-Gutiérrez S, Silla-Martínez JM, Gabaldón T. trimAl: a tool for automated alignment
732 trimming in large-scale phylogenetic analyses. Bioinformatics. 2009;25: 1972–1973.
733 doi:10.1093/bioinformatics/btp348

734 77. Tamura K, Stecher G, Kumar S. MEGA11: Molecular Evolutionary Genetics Analysis
735 Version 11. Mol Biol Evol. 2021;38: 3022–3027. doi:10.1093/molbev/msab120

736 78. Guindon S, Dufayard J-F, Lefort V, Anisimova M, Hordijk W, Gascuel O. New algorithms
737 and methods to estimate maximum-likelihood phylogenies: assessing the performance of
738 PhyML 3.0. Syst Biol. 2010;59: 307–321. doi:10.1093/sysbio/syq010

739 79. Le SQ, Gascuel O. An Improved General Amino Acid Replacement Matrix. Molecular
740 Biology and Evolution. 2008;25: 1307–1320. doi:10.1093/molbev/msn067

741 80. Teufel F, Almagro Armenteros JJ, Johansen AR, Gíslason MH, Pihl SI, Tsirigos KD, et al.
742 SignalP 6.0 predicts all five types of signal peptides using protein language models. Nat
743 Biotechnol. 2022;40: 1023–1025. doi:10.1038/s41587-021-01156-3

744 81. Macke TJ, Ecker DJ, Gutell RR, Gautheret D, Case DA, Sampath R. RNAMotif, an RNA
745 secondary structure definition and search algorithm. Nucleic Acids Research. 2001;29:
746 4724–4735. doi:10.1093/nar/29.22.4724

747 82. Gautheret D, Lambert A. Direct RNA motif definition and identification from multiple
748 sequence alignments using secondary structure profiles. Journal of Molecular Biology.
749 2001;313: 1003–1011. doi:10.1006/jmbi.2001.5102

750 83. Li X, Xie Y, Liu M, Tai C, Sun J, Deng Z, et al. oriTfinder: a web-based tool for the
751 identification of origin of transfers in DNA sequences of bacterial mobile genetic elements.
752 Nucleic Acids Res. 2018;46: W229–W234. doi:10.1093/nar/gky352

753 84. Kent WJ, Sugnet CW, Furey TS, Roskin KM, Pringle TH, Zahler AM, et al. The Human
754 Genome Browser at UCSC. Genome Res. 2002;12: 996–1006. doi:10.1101/gr.229102

755

756

757 **Fig 1. Identification of an additional IncC exclusion factor.** (A) Overview of the TnSeq
758 workflow to identify exclusion factors in pVCR94^{Kn} Δ*eexC*::*cat*. (B) Mini-Tn5 reads in the vicinity
759 of *vcrx085*. The tracks plot the number of reads from two independent replicates as a function of
760 position in pVCR94^{Kn} Δ*eexC*::*cat* for both the input and output libraries. ORFs with similar
761 functions are colour-coded as indicated in the panel. (C) Nine loci of unknown function show a
762 mini-Tn*5* insertion index ratio greater than 5 (dashed line), calculated as the ratio of insertion
763 counts between the output and input libraries. ORFs with similar functions are colour-coded as
764 indicated in Fig S1. (D) *sfx* (*vcrx085*) is the only functional exclusion factor among candidates
765 identified in (B) and suffices alongside *eexC* (*eex*) to account for the totality of IncC exclusion.
766 *E. coli* VB112 containing pVCR94^{Kn} and pClo served as the donor strain, and *E. coli* GG56
767 containing the specified derivatives of pVCR94^{Sp} served as the recipient strains. When
768 indicated, *eexC* or *sfx* were expressed from single-copy, chromosomally integrated pAH56 in
769 the recipients in the presence of IPTG. Transconjugants containing pClo were selected as the
770 Nx^{r} Ap^{r} colonies. This figure was created using the UCSC Genome Browser
771 (http://genome.ucsc.edu).
772 **Fig 2. Expression of IncC surface exclusion is independent of the master activator of**
773 **transfer AcaCD.** (A) and (B) Cell fractionation assay. The total cell extract (T) and outer
774 membrane fraction (OM) from *E. coli* BL21 expressing a 3xFLAG-tagged Sfx$_{94}$ were analyzed
775 by SDS-PAGE and stained with Coomassie blue (A) or immunodetected using an anti-FLAG
776 antibody (B). Molecular weight markers (M) are indicated on the left. A vertical white line
777 separates non-adjacent lanes from a single gel or blot. (C) Schematic representation of the
778 *acaB-sfx* locus. The relative positions of reverse transcription primer 85RT and primers used to
779 amplify *sfx* and *acaB* are shown. A dotted line shows the reverse transcription product. Stem
780 loops represent predicted Rho-independent terminators. (D) *sfx* is expressed constitutively and

781 independently of the upstream AcaCD-dependent P_{acaB} promoter. A 2% agarose gel of the PCR
782 products from an *sfx*-derived reverse transcribed RNA. Untreated RNA (RNA) and genomic
783 DNA from *E. coli* GG56 containing pVCR94^{Kn} Δ*acaCD* (gDNA) were used as negative and
784 positive controls, respectively. β-galactosidase activity of GG56 containing pVCR94^{Kn} *eexC'-*
785 *'lacZ* or pVCR94^{Kn} *sfx'-'lacZ* transcriptional fusions with or without p*acaCD* and arabinose on
786 agar medium (E) or in quantitative enzymatic assays (F).
787 **Fig 3. Sfx homologs are found across a wide range of Gammaproteobacteria.** Maximum
788 likelihood phylogenetic analyses of Sfx (A) and TraN (B) homologs. Trees with the highest
789 likelihood (9,621.78 and 28,204.23 for Sfx and TraN, respectively) are shown. Bootstrap
790 supports are indicated as percentages at the branching points only when >80%. Branch lengths
791 represent the number of substitutions per site over 269 and 813 amino acid positions for Sfx
792 and TraN, respectively. Only one representative per cluster of similar proteins (>90%) is shown
793 in each tree, except for $TraN_{Asa4c}$ and $TraN_{AhD4-1}$, which share 95% identity over the aligned
794 sequences. S5 Table provides additional details on host strains. (C) Schematic representation
795 of the genetic context of *sfx* homologs in a selection of putative IMEs and ACL plasmids.
796 Predicted *attL* and *attR* attachment sites flanking the IMEs are represented by blue bars.
797 pAQU1 encodes homologs of *acaB*, *vcrx087-088-089-090*, *bet* and *exo* clustered in a distinct
798 locus not shown here. ORFs with similar functions are colour-coded as indicated in the panel.
799 **Fig 4. TraN directs surface exclusion specificity.** (A) The presence of *eexC* and *sfx* in the
800 donor decreases the frequency of transconjugant formation. pClo was mobilized from *E. coli*
801 VB112 bearing the indicated deletion mutants of pVCR94^{Sp} (donor) into *E. coli* GG56 bearing
802 pVCR94^{Kn} (recipient). Transconjugants containing pClo were selected as the Nx^r Ap^r colonies.
803 (B) sfx_{94} is ineffective against the $traN_{94}$ distant homolog $traN_{AQU1}$. (C) Heatmap of surface
804 exclusion indices of *sfx* and *traN* pairs from a diverse set of ACL plasmids. In (B) and (C), *E. coli*

805 GG56 containing pVCR94^{Sp} Δ*traN* and expressing the indicated *traN* variant from pBAD30
806 served as the donor, and *E. coli* CAG18439 expressing the indicated *sfx* variant from a single-
807 copy, chromosomally integrated pAH56 was used as the recipient. Transconjugants containing
808 pVCR94^{Sp} Δ*traN* were selected as the Tc^{r} Sp^{r} colonies.
809

810 **Supporting information**

811 **S1 Fig. Identification of an additional IncC exclusion factor by TraDIS.** The tracks plot the
812 number of reads from two independent replicates as a function of position in pVCR94^{Kn}
813 Δ*eexC*::*cat* for both the input and output libraries. ORFs with similar functions are colour-coded
814 as indicated in the figure. This figure was created using the UCSC Genome Browser
815 (http://genome.ucsc.edu).
816 **S2 Fig. Sfx is a predicted lipoprotein.** (A) Schematic representation of the predicted
817 translation products of sfx_{94} and $traN_{94}$ and their predicted signal peptide sequences. (B)
818 Predicted Rho-independent terminators in the proximity of *sfx* in the IncC plasmid pVCR94.
819 Terminator sequences are provided with the stems and loops in blue and red, respectively.
820 Their position is represented by hairpins on the schematic representation of the region.
821 Predicted ΔG values are indicated in kcal/mol.
822 **S3 Fig. Sequence identity heatmap showing pairwise percentage identity between 18**
823 **selected Sfx homologs.** Panels are shaded as indicated in the Figure according to the identity
824 calculated for each pair.
825 **S4 Fig. TraN directs surface exclusion specificity.** *E. coli* GG56 containing pVCR94^{Sp} Δ*traN*
826 and expressing the indicated *traN* variants from pBAD30 served as the donor, and *E. coli*
827 CAG18439 expressing the indicated *sfx* variants from a single-copy, chromosomally integrated

828 pAH56 was used as the recipient. Transconjugants containing pVCR94^{Sp} Δ*traN* were selected

829 as the Tc^{r} Sp^{r} colonies.

830 **S1 Table. Primers used in this study.**

831 **S2 Table. Strains and plasmids used in this study.**

832 **S3 Table. Predicted AcaCD binding sites.**

833 **S1 File. Complete data sets.**

834 **S2 File. Statistical analyses.**

835 **S3 File. Sfx and TraN homologs.**

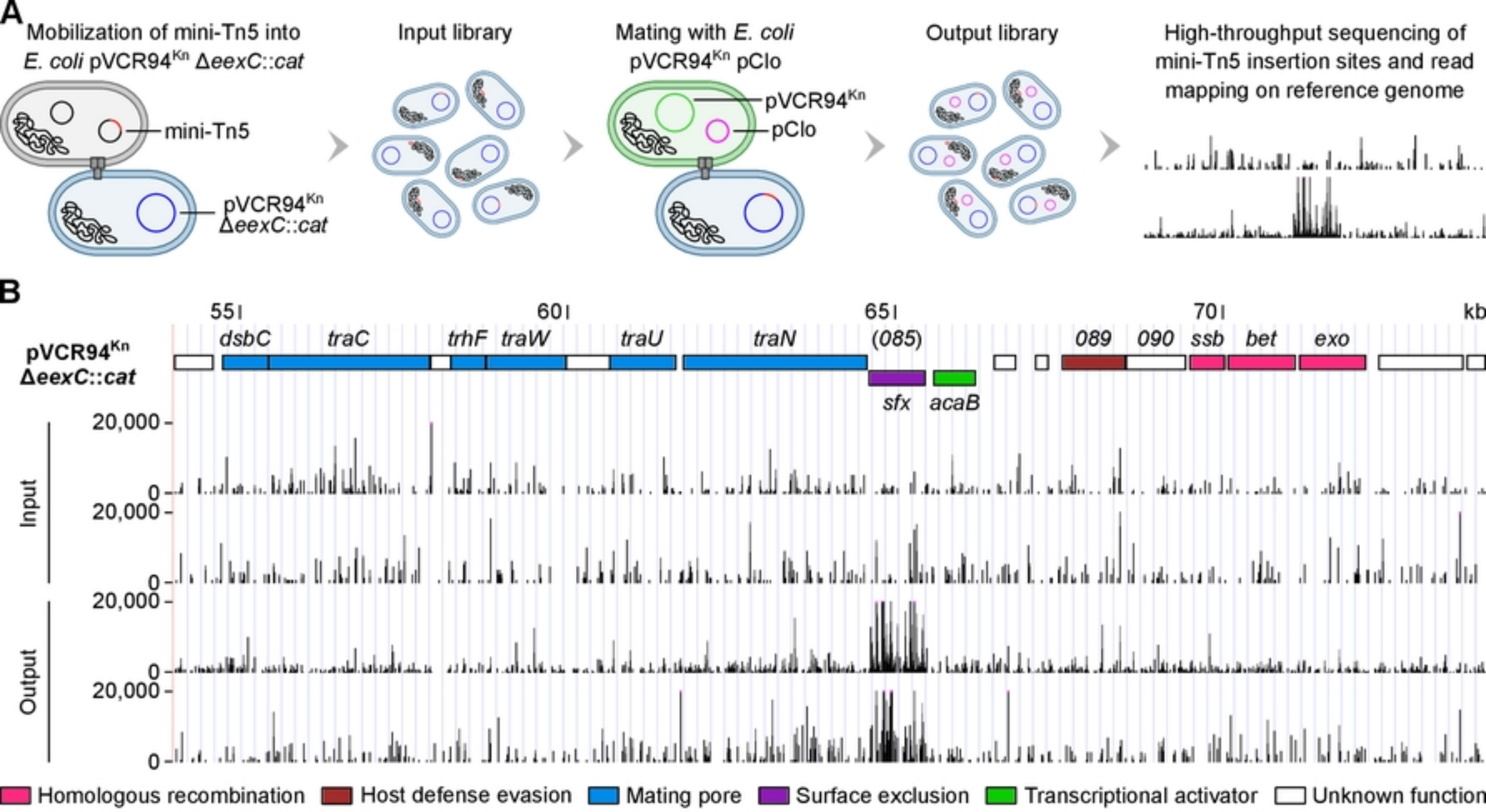
A
Mobilization of mini-Tn5 into E. coli pVCR94Kn ΔeexC::cat
mini-Tn5
pVCR94Kn ΔeexC::cat
Input library
Mating with E. coli pVCR94Kn pClo
pVCR94Kn
pClo
Output library
High-throughput sequencing of mini-Tn5 insertion sites and read mapping on reference genome
B
pVCR94Kn ΔeexC::cat
dsbC
traC
trhF
traW
traU
traN
(085)
089
090
ssb
bet
exo
sfx
acaB
Input
Output
Homologous recombination
Host defense evasion
Mating pore
Surface exclusion
Transcriptional activator
Unknown function
C
Insertion index ratio (output/input)
Relative position
062
018
019
085
107
108
111
137
acr2
D
Log10(transconjugants/donor)
Anova, p=8e−24
pVCR94Sp
pAH56
WT
018 -019
062
107 -108
111
137
acr2
sfx
eex
eex sfx

Figure 1

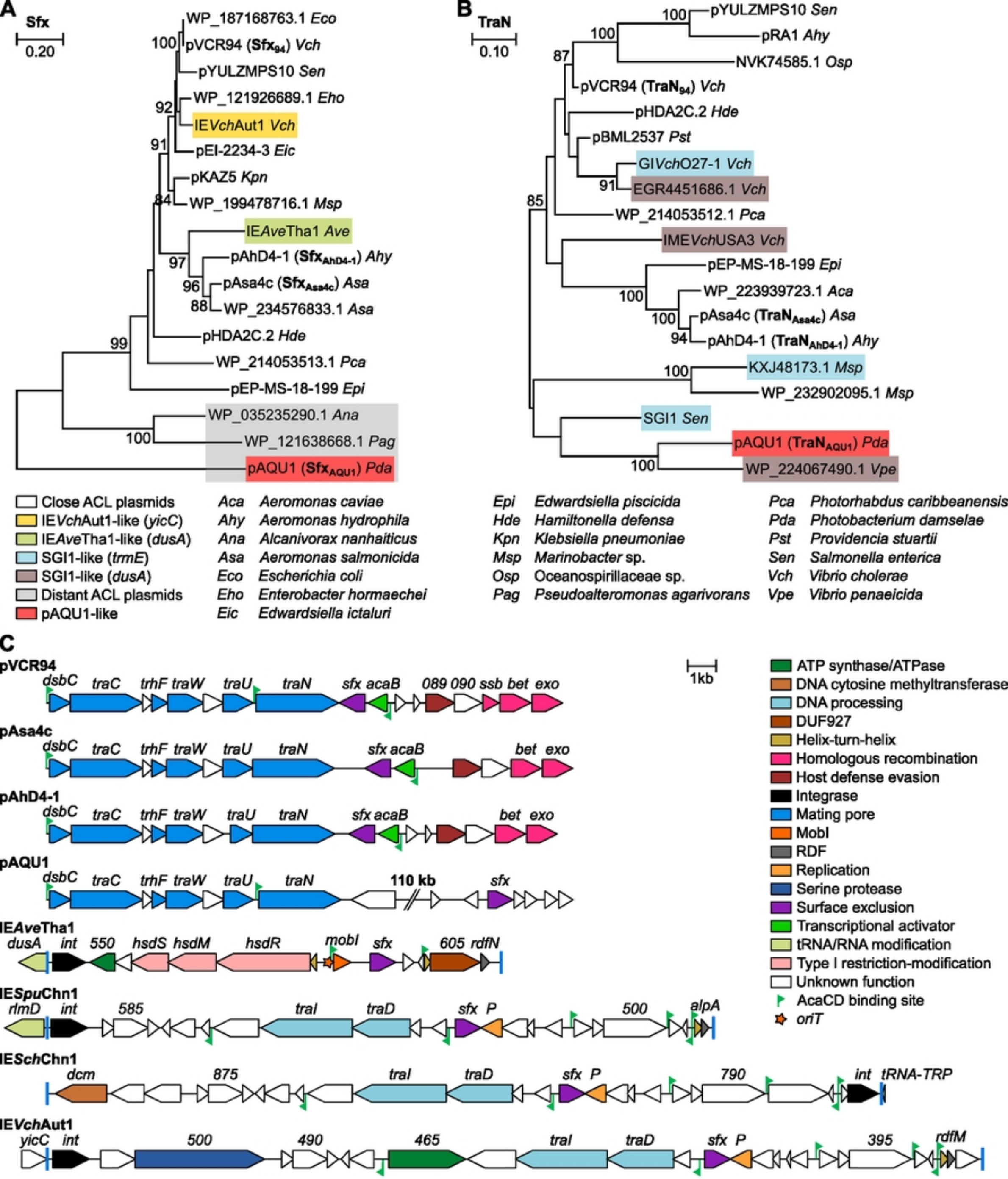
A
Sfx
0.20
WP_187168763.1 Eco
pVCR94 (Sfx94) Vch
pYULZMPS10 Sen
WP_121926689.1 Eho
IEVchAut1 Vch
pEI-2234-3 Eic
pKAZ5 Kpn
WP_199478716.1 Msp
IEAveTha1 Ave
pAhD4-1 (SfxAhD4-1) Ahy
pAsa4c (SfxAsa4c) Asa
WP_234576833.1 Asa
pHDA2C.2 Hde
WP_214053513.1 Pca
pEP-MS-18-199 Epi
WP_035235290.1 Ana
WP_121638668.1 Pag
pAQU1 (SfxAQU1) Pda
B
TraN
0.10
pYULZMPS10 Sen
pRA1 Ahy
NVK74585.1 Osp
pVCR94 (TraN94) Vch
pHDA2C.2 Hde
pBML2537 Pst
GIVchO27-1 Vch
EGR4451686.1 Vch
WP_214053512.1 Pca
IMEVchUSA3 Vch
pEP-MS-18-199 Epi
WP_223939723.1 Aca
pAsa4c (TraNAsa4c) Asa
pAhD4-1 (TraNAhD4-1) Ahy
KXJ48173.1 Msp
WP_232902095.1 Msp
SGI1 Sen
pAQU1 (TraNAQU1) Pda
WP_224067490.1 Vpe
Close ACL plasmids
IEVchAut1-like (yicC)
IEAveTha1-like (dusA)
SGI1-like (trmE)
SGI1-like (dusA)
Distant ACL plasmids
pAQU1-like
Aca Aeromonas caviae
Ahy Aeromonas hydrophila
Ana Alcanivorax nanhaiticus
Asa Aeromonas salmonicida
Eco Escherichia coli
Eho Enterobacter hormaechei
Eic Edwardsiella ictaluri
Epi Edwardsiella piscicida
Hde Hamiltonella defensa
Kpn Klebsiella pneumoniae
Msp Marinobacter sp.
Osp Oceanospirillaceae sp.
Pag Pseudoalteromonas agarivorans
Pca Photorhabdus caribbeanensis
Pda Photobacterium damselae
Pst Providencia stuartii
Sen Salmonella enterica
Vch Vibrio cholerae
Vpe Vibrio penaeicida
C
pVCR94
dsbC traC trhF traW traU traN sfx acaB 089 090 ssb bet exo
pAsa4c
dsbC traC trhF traW traU traN sfx acaB bet exo
pAhD4-1
dsbC traC trhF traW traU traN sfx acaB bet exo
pAQU1
dsbC traC trhF traW traU traN 110 kb sfx
IEAveTha1
dusA int 550 hsdS hsdM hsdR mobI sfx 605 rdfN
IESpuChn1
rlmD int 585 traI traD sfx P 500 alpA
IESchChn1
dcm 875 traI traD sfx P 790 int tRNA-TRP
IEVchAut1
yicC int 500 490 465 traI traD sfx P 395 rdfM
1kb
ATP synthase/ATPase
DNA cytosine methyltransferase
DNA processing
DUF927
Helix-turn-helix
Homologous recombination
Host defense evasion
Integrase
Mating pore
MobI
RDF
Replication
Serine protease
Surface exclusion
Transcriptional activator
tRNA/RNA modification
Type I restriction-modification
Unknown function
AcaCD binding site
oriT

Figure 3

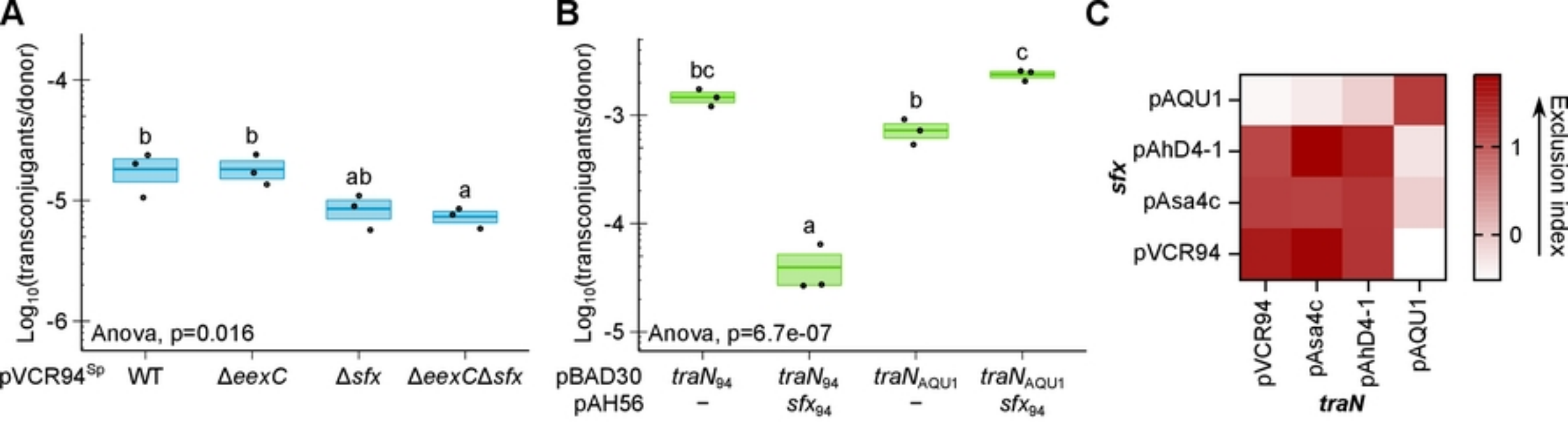
A
Log10(transconjugants/donor)
-4
-5
-6
b
b
ab
a
Anova, p=0.016
pVCR94Sp
WT
ΔeexC
Δsfx
ΔeexCΔsfx
B
Log10(transconjugants/donor)
-3
-4
-5
bc
a
b
c
Anova, p=6.7e-07
pBAD30
pAH56
traN94
–
traN94
sfx94
traNAQU1
–
traNAQU1
sfx94
C
sfx
pAQU1
pAhD4-1
pAsa4c
pVCR94
traN
pVCR94
pAsa4c
pAhD4-1
pAQU1
1
0
Exclusion index

Figure 4

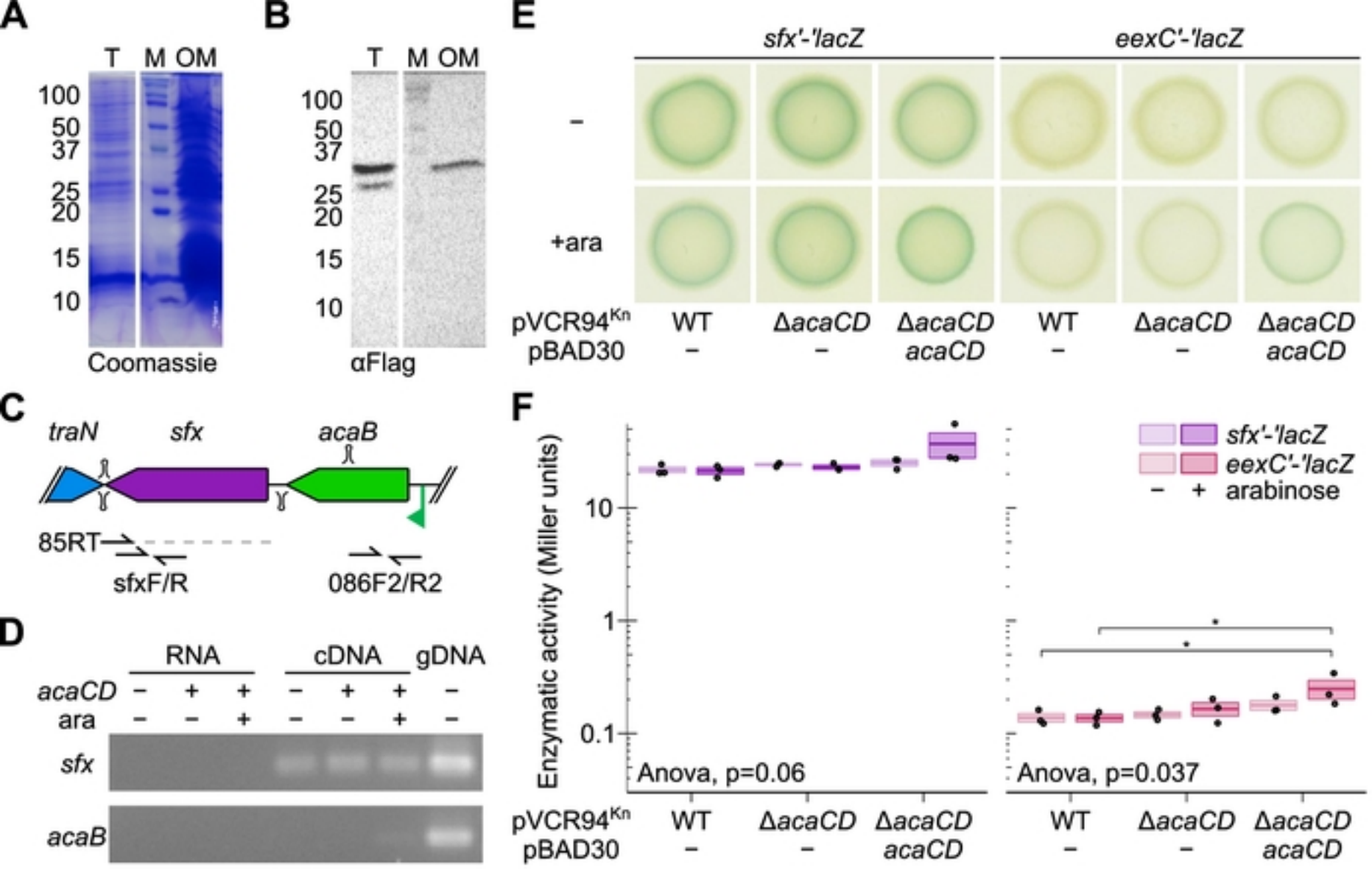
A
T M OM
100
50
37
25
20
15
10
Coomassie
B
T M OM
100
50
37
25
20
15
10
αFlag
C
traN
sfx
acaB
85RT
sfxF/R
086F2/R2
D
RNA
cDNA
gDNA
acaCD
ara
sfx
acaB
E
sfx'-'lacZ
eexC'-'lacZ
–
+ara
pVCR94Kn
pBAD30
WT
ΔacaCD
ΔacaCD acaCD
F
Enzymatic activity (Miller units)
sfx'-'lacZ
eexC'-'lacZ
– + arabinose
Anova, p=0.06
Anova, p=0.037

Figure 2